



Universidad  
Carlos III de Madrid



This is a print version of the following published document:

C. Vázquez, A. Tapetado, J. Orcutt, H. C. Meng, R. Ram. Tolerance analysis for efficient MMI devices in silicon photonics. Silicon Photonics IX" conference. *Proc. of SPIE (2014)* Vol.89900 pp: 89900A-89900A-7. Available in <http://www.dx.doi.org/10.1117/12.2039730>

© SPIE 2014. One print or electronic copy may be made for personal use only. Systematic electronic or print reproduction and distribution, duplication of any material in this paper for a fee or for commercial purposes, or modification of the content of the paper are prohibited.

# Tolerance analysis for efficient MMI devices in silicon photonics

Carmen Vázquez<sup>a,b</sup>, Alberto Tapetado<sup>a,b</sup>, Jason Orcutt<sup>b</sup>, Huaiyu Charles Meng<sup>b</sup>, Rajeev Ram<sup>b</sup>  
<sup>a</sup>Grupo de Displays y Aplicaciones Fotónicas, Dept. Tecnología Electrónica, Universidad Carlos III  
Madrid, Av. Universidad 30, 28911 Leganés, Madrid, Spain;  
<sup>b</sup>Physical Optics and Electronics Group, Research Laboratory of Electronics, Massachusetts  
Institute of Technology, 77 Massachusetts Av, MA 02139, USA;

## ABSTRACT

Silicon is considered a promising platform for photonic integrated circuits as they can be fabricated in state-of-the-art electronics foundries with integrated CMOS electronics. While much of the existing work on CMOS photonics has used directional couplers for power splitting, multimode interference (MMI) devices may have relaxed fabrication requirements and smaller footprints, potentially energy efficient designs. They have already been used as 1x2 splitters, 2x1 combiners in Quadrature Phase Shift Keying modulators, and 3-dB couplers among others. In this work, 3-dB, butterfly and cross MMI couplers are realized on bulk CMOS technology. Footprints from around 40 $\mu\text{m}^2$  to 200  $\mu\text{m}^2$  are obtained. MMI tolerances to manufacturing process and bandwidth are analyzed and tested showing the robustness of the MMI devices.

**Keywords:** power efficiency, multimode interference couplers, silicon photonics, manufacturing tolerances, CMOS photonics, post-manufacturing trimming, integrated optic devices

## 1. INTRODUCTION

Silicon is considered a promising platform for photonic integrated circuits (PIC) as PICs can be fabricated in state-of-the-art electronics foundries with integrated CMOS electronics [1], [2]. Besides, the high index contrast between silicon or polysilicon and silicon dioxide allows manufacturing waveguides with submicron cross sections and very small bending radii, leading to high integration density. While much of the existing work on CMOS photonics [1][2] has used directional couplers for power splitting, multimode interference (MMI) devices may have relaxed fabrication requirements and smaller footprints [3] compared to other configurations based on coupling between parallel waveguides, potentially energy efficient designs. MMI devices have already been used as 1x2 splitters, 2x1 combiners in Quadrature Phase Shift Keying (QPSK) modulators [4], 3-dB couplers in ring resonators [5] and cross couplers for switches [6][7]. State-of-the-art CMOS manufacturing processes have nanometer scale lithographic precision. In contrast, the lower resolution photolithography available for InP devices coupled with the precision of epitaxial growth results in the device width being the most variable dimension in InP [3], meanwhile CMOS layer thicknesses is less accurately controlled than InP epitaxial film thickness.

In this work, 3-dB, butterfly and cross-MMI couplers, based on silicon waveguides are realized on bulk CMOS technology [2]. Footprints from around 40 $\mu\text{m}^2$  to 200  $\mu\text{m}^2$  are obtained for the different devices. MMI tolerances to manufacturing process and bandwidth are analyzed and tested showing the robustness of the MMI devices. Due to the high contrast ratio of these waveguides 3D-FDTD simulations are performed to get accurate designs [8].

## 2. THEORY

General NxN MMI couplers are made of a multimode section of width  $W$  or  $W_{MMI}$ . Those devices have  $N$  self-images of equal intensities  $1/N$  at the length  $L_{MN}$ . For  $N=1$  an image will appear symmetrically placed versus the input, and the device will behave as a cross coupler. The length  $L_{MN} = N/M 3Lc$ , being  $Lc$  the coupling length between the fundamental and first order guided modes, is given by

$$L_c = \frac{4n_{eff} \times W_{eq}^2}{3\lambda} \quad (1)$$

Being  $\lambda$  the wavelength in vacuum,  $n_{eff}$  the effective refractive index and  $W_{eq}$  is close to  $W$ , strictly speaking is the equivalent MMI width, which is the geometric width of the MMI section including the penetration into the neighbor material of the waveguide.

By placing input and output waveguides at specific positions, images that were far apart can overlap; the reduced number of images after overlapping is usually called  $K$ . These new MMI devices with overlapping images are named *overlapping MMI devices* and the equations describing their behavior in a general form (intensities and phases at different positions) can be found in [9]. A specific example of an overlapping MMI device is named by some authors as restricted interference MMI coupler [10] or paired interference coupler [11]. These devices provide wider MMI devices with shorter lengths for the same behavior, typically a 50/50 (or 3-dB), cross or bar coupler. Overlapping MMI devices can also be designed to behave as couplers with different splitting ratios between the outputs. In the following (see Fig. 1.a), it can be seen the structure of those devices in the  $i+j$  even case,  $i$  refers to the input and  $j$  to the output, as an example. It can be seen that the input and output waveguides are placed at locations defined by  $W/N$ . Only specific splitting ratios can be obtained with these devices.

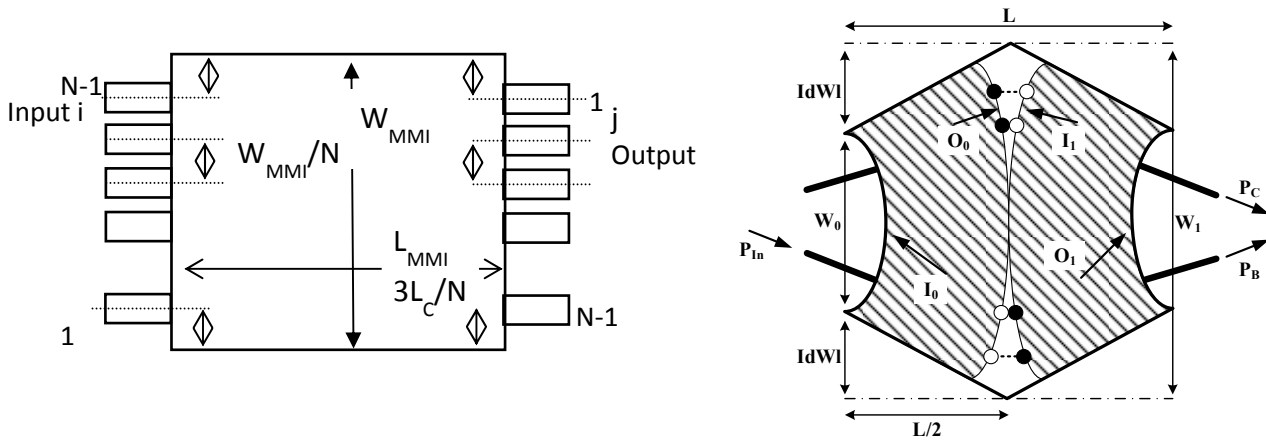


Fig. 1. (a) Overlapping-Image MMI coupler

(b) Butterfly up-tapered MMI coupler

Butterfly configurations were proposed by Besse [12] as a way to design MMI devices with arbitrary power splitting ratio, not fixed only to the overlap-type [9]. By transforming the rectangular geometry of standard MMI devices into a series of down- and up-tapered profiles, ultra-compact phase shifters are introduced in the components. The device length depends on the depth of the tapered profile as

$$L_{c\ BUT} \cong \frac{4n_{eff}}{3} \frac{W_o W_1}{\lambda} \quad (2)$$

being  $W_o$  and  $W_1$  the extreme and center width of the MMI section respectively, and the other parameters are those already defined in Eq. (1).

There are different configurations, but we only report here one of them. The butterfly MMI coupler with symmetric up-tapered profile, excited at  $W_o/3$  and  $2W_o/3$ , with a length  $L_c$ ; a mixture between the configurations A and B defined in [12].  $dW=W_o/2$  for  $W_1=2W_o$  and from Eq. (2)  $L_{c\ BUT}=2L_c$  so the butterfly MMI coupler with length  $L_c$  will behave as a bar coupler with half the length.

## 2.1 Tolerance analysis of MMI couplers

In this work, we proposed the analysis of general and overlap-type MMI device tolerance to manufacturing deviations in CMOS photonics. The effective refractive index variations due to growth process are expected to change the splitting ratio from the optimum MMI device design. The selected MMI devices are as shorter as possible, as they are expected to be more tolerant to manufacturing deviations as it will be briefly described in this section.

MMI tolerance analysis using an analytical approach based on a 2D approximation and measurements on InP based devices are reported in [3] and [13]. From Eq.(1) the variations of the wavelength, the width, the effective refractive index and the length of the MMI coupler are related by

$$\frac{\partial L}{L} = \frac{2\partial W}{W} = \frac{\partial n_{eff}}{n_{eff}} = \left| \frac{\partial \lambda}{\lambda} \right| \quad (3)$$

From Eq. (3) it can be directly inferred that shorter devices will be more tolerant so higher losses and smaller fabrication tolerances are expected for a cross-coupler compare to a 3dB MMI coupler.

For well-separated output images, any design parameter variation leads first to an increase of the losses, so the optical bandwidth and the fabrication tolerances can be described in terms of excess losses,  $\alpha$ . The excess losses are calculated as a function of the MMI length variation; the optical field amplitude of the single mode symmetrical input and output waveguides are approximated by Gaussian beams of waist  $d_o$ . This MMI length variation is given by

$$\partial L \leq Z(\alpha) d_o^2 \frac{\pi n_{eff}}{\lambda} \quad (4)$$

where  $Z(\alpha)$  is a function of the excess loss described in [3]. They also choose to express the fabrication tolerances by the width variation since this geometrical parameter is the most critical for InP manufacturing process. But this is not the case in state-of-the-art CMOS manufacturing processes with nanometer scale lithographic precision. Instead, CMOS layer thicknesses is less accurately controlled than InP epitaxial film thickness, and consequently the fabrication tolerances should be expressed by the effective refractive index variations. Introducing the result of Eq. (4) in Eq. (3) and being  $L = L_{MN} = N/M 3Lc$ , we get the fabrication tolerances

$$\partial n_{eff} \leq Z(\alpha) \frac{d_o^2}{W^2} n_{eff} a \frac{\pi N}{8M} \quad (5)$$

As expected, the manufacturing tolerances are proportional to the square of the ratio between the beam waist and the MMI section width or normalized access waveguide width. For general interference MMI couplers (GI),  $a$  is equal to 1 and for restricted interference couplers (RI),  $a$  is equal to 3.

Using the same procedure, it can be seen that the optical bandwidth is also proportional to the square of the normalized access waveguide width.

In summary, shorter devices with higher normalized access waveguide widths will be more robust to manufacturing tolerances and will have higher optical bandwidth, if excess loss rather than imbalance is the optimized parameter. Another expressions based on a 2D approximation for optimizing imbalance and loss in 2x2 3dB MMI couplers via access waveguide width are reported in [14]. It is also shown that obtaining the lowest loss requires choosing the largest possible access waveguide width and that a reduced number of modes does not affect significantly for large normalized access waveguide width. On the other hand, the imbalance does not decrease monolithically with the normalized access waveguide width.

Previous approximations are good to get general conclusions about the expected tolerance behavior of MMI couplers, but for specific designs neither 2D approximations or 3D BPM analysis are accurate enough for a high index contrast system [15] [8]; instead 3D Finite Difference software, 3D FDTD Fullwave, will be used to find the imaging position and evaluate the device performance. In the case of the butterfly MMI couplers other full-vectorial mode expansion software based on the mode matching method can neither be easily used because of the propagation variation of the MMI section width and consequently the number of modes and vector base variation along propagation. 3D calculations of coupling behavior and loss in MMI devices for accurate results were also performed in [16]. It was shown that for increasing total number of modes in the MMI section, the loss increase due to the larger geometrical mismatch, as shown

in Eq. (5), is stronger than the loss decreases due to the larger number of modes in the MMI section. The imbalance is adjusted by the input waveguides offset.

## 2.2 MMI couplers design in CMOS processes

The tape-outs are designed for a specific bulk CMOS process so the different layer thickness and material composition are fixed. A detailed description of the process allowing integrating photonic devices with electronic components can be shown in [1] [2]. The operation design wavelength is 1550nm. The polysilicon gate is used as the waveguide core (see Fig. 2.a) which is surrounded by a  $\text{Si}_3\text{N}_4$  conformal layer. The cladding is formed by  $\text{SiO}_2$ . In this process the thickness of the polysilicon layer is 225nm. The waveguides are designed for a barely single mode operation and minimizing bending loss. In this case the width is 440nm. It has been defined a multilayer structure in RSoft platform. FemSim software is used for calculating the access input waveguide component fields and propagation constants of the waveguides and MMI section modes. 3D FDTD Fullwave software is used for calculating the field components on the MMI devices to determine their free design dimensions. Different MMI devices, 3dB couplers, cross couplers and butterfly bar couplers are designed for achieving higher manufacturing tolerances so with the shortest lengths and highest normalized access waveguide widths. A minimum separation of 500 nm between core access waveguides is considered to avoid crosstalk. 3 dB RI and GI MMI couplers with almost the same length are designed to make a comparison between both configurations. A different set of MMI cross couplers are included in the tape-out, with  $W_{\text{MMI}}=1.8\mu\text{m}$  and  $W_{\text{MMI}}=3.6\mu\text{m}$ , in the case of the butterfly MMI couplers the centre width is  $2W_{\text{MMI}}$ . Tapers are included at the input and output ports to reduce excess losses and increase the normalized access waveguide widths on RI MMI configurations. For each device, 3 different lengths are considered. Schematics of the top view of the designed devices are shown in Fig. 2, all dimensions are in microns.

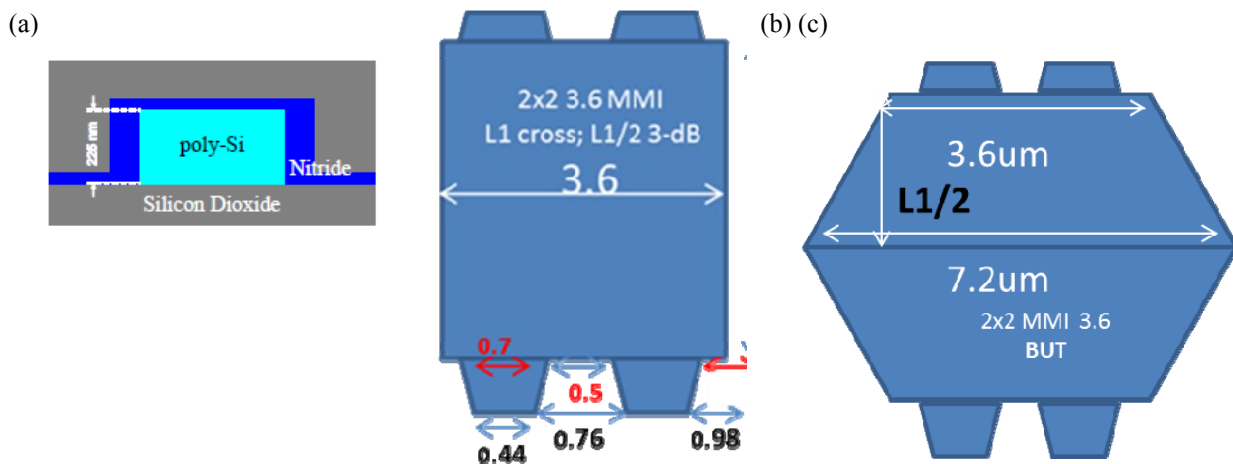


Fig. 2. (a) Schematic of waveguide structure (b) MMI 3dB and cross RI coupler (c) MMI butterfly bar coupler

## 3. EXPERIMENTS

A detailed description of the bulk CMOS process used in manufacturing the MMI devices in a monolithic front-end integration platform that enables electronic-photonic integrated circuit fabrication can be seen in [2]. Photonic devices were defined using the standard electronic process design kit layers in Cadence Virtuoso, a common VLSI electronics CAD environment (a Cadence lay-out screen shot of a butterfly MMI coupler is shown in Fig. 3(a)). Different test structures are included in the same wafer, some of them with contacts (see Fig. 3.b).

Grating couplers provide surface-normal optical input and output for MMI devices. Optimum coupling for specific wavelength range is achieved by using a vertically-coupled test platform with input/output SMF-28e fibers at a fix angle relative to the normal surface (see Fig. 3 (c)) to match the mode size of the grating couplers. 10% input power is monitored to test the source performance, and to take a reference measurement. A tunable laser source is used for measuring the excess loss and imbalance versus wavelength as a test of the MMI device tolerance. From Eq. (3) greater tolerance on optical bandwidths can imply greater manufacturing tolerances.

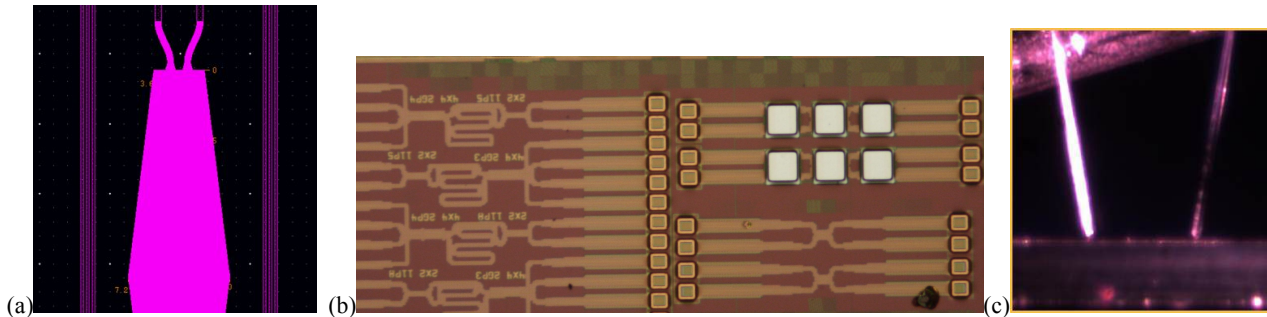


Fig. 3 (a) Cadence lay-out of a butterfly MMI coupler (b) Photograph of array test structures in the manufactured chip (c) Input/output angled optical fibers to the chip surface on the test platform.

### 3.1 Measurements and discussion

Output power of MMI devices have been characterized from 1530 to 1570nm. Single waveguides with input/output grating couplers and bends are also characterized on the same chip for reference purposes. In Fig. 4.a output power measurements and imbalance of a GI 3dB MMI coupler with a footprint of  $1.8 \times 1.5 \mu\text{m}^2$  are reported.

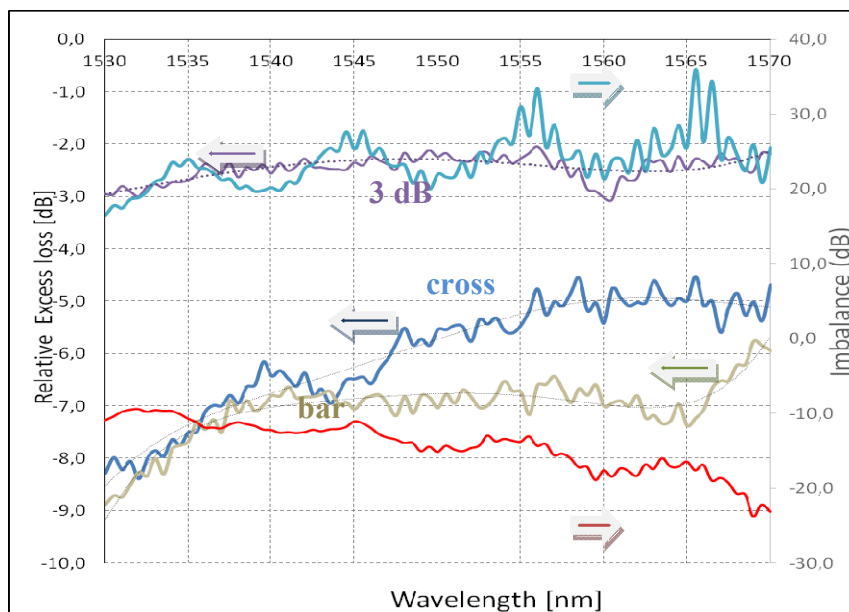
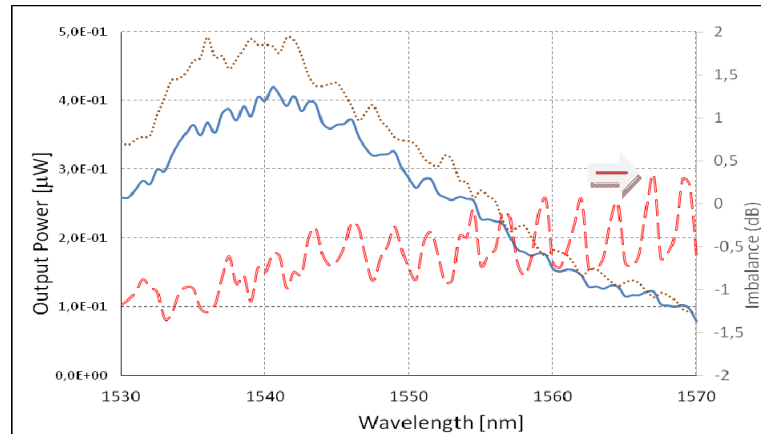


Fig. 4 (a) Power measurements (... cross output, \_\_\_\_ bar output) and imbalance (---) versus wavelength for a 3dB MMI coupler. (b) Comparison of excess loss and imbalance optical bandwidth versus wavelength for different MMI couplers.

A summary of the results on 3dB MMI couplers can be seen on Table 1. The wavelength range (BW) for a certain excess loss (EL) increment is used as the figure of merit to determine the device tolerance. GI MMI coupler with a slightly shorter length and greater normalized access waveguides is a bit more tolerant as expected. A high index contrast MMI coupler of 1.8 $\mu\text{m}$  width can support 12 modes, meanwhile MMI couplers of 3.6 $\mu\text{m}$  width can support up to 21 modes. EL increments below 0.5dB can be obtained within a range of 36nm for both GI and RI MMI couplers. Using a mode solver it is estimated that a layer thickness variation from 215nm to 235nm is responsible of a normalized index change on the MMI section fundamental mode of around 0.025 at 1550nm, meanwhile a wavelength variation of 40nm from 1530 to 1570nm is responsible of a normalized index change on the MMI section fundamental mode of around 0.006. Having in mind the relation between optical bandwidth and manufactured tolerances shown on Eq. (3), EL increments can be expected if there are layer thickness tolerances of around 5%. In terms of imbalance, defined as the output powers ratio in dB, higher tolerances are also obtained for the more compact coupler, with values below 1dB in s 35nm range. This 40nm optical bandwidth is within the range of recently reported 1x2 MMI splitters on silicon-on-insulator with 0.13 $\mu\text{m}$  technology, for 0.1dB excess loss [15] and  $3.6 \times 11.5 \mu\text{m}^2$ , although with the same MMI section, the length should be twice to get a 2x2 3dB coupler.

Table 1. Optical bandwidth (BW) from Excess Loss (EL) at  $\lambda_0=1550\text{nm}$  for different 3dB MMI couplers

Interference mechanism	$W_{\text{MMI}}$ (um)	$L_{\text{MMI}}$ (um)	BW (nm)		BW (nm) Imbalance <1dB
			EL increment* <0.1dB	EL increment* <0.5dB	
GI	1.8	11.3	4	40	33
<b>GI</b>	<b>1.8</b>	<b>11.5</b>	<b>20</b>	<b>40</b>	<b>35</b>
GI	1.8	11.7	15	29	32
<b>RI</b>	<b>3.6</b>	<b>14.7</b>	<b>11.5</b>	<b>36</b>	<b>25</b>
RI	3.6	14.8	10	32	12

Cross MMI couplers with a footprint of  $3.6 \times 29.6 \mu\text{m}^2$  and bar butterfly MMI couplers with footprints of  $7.2 \times 29.6 \mu\text{m}^2$  are also manufactured and they have been characterized in terms of excess loss and imbalance versus wavelength. Both are based on restricted interference configurations. Results can be shown on Table 2 and on Fig. 4.b.

Table 2. Optical bandwidth (BW) from Excess Loss (EL) at  $\lambda_0=1550\text{nm}$  for different cross and butterfly MMI couplers. <sup>1</sup> Butterfly MMI has  $W_0=W_{\text{MMI}}$  and  $W_1=7.2 \mu\text{m}$

MMI coupler type	$W_{\text{MMI}}$ (um) <sup>1</sup>	$L_{\text{MMI}}$ (um)	BW (nm)		BW (nm) Imbalance <15dB	
			EL increment* <0.5dB			
Cross/ butterfly bar	3.6	29.4	6	29	-	40
Cross/ butterfly bar	3.6	29.6	7.5	25	7.5	40
Cross/ butterfly bar	3.6	29.8	13	30	13	40

Optical bandwidths are smaller than in shorter 3dB couplers with the same normalized access waveguides. On the other hand, butterfly bar couplers although having a higher excess loss are more tolerant than cross couplers. They also have better imbalance in the whole wavelength range. These butterfly MMI bar couplers are shorter than others based on conventional MMI couplers with twice the MMI section length.

#### 4. CONCLUSIONS

Small footprints 3-dB, bar and cross multimode interference couplers based on silicon waveguides are realized on bulk CMOS technology. It has been demonstrated that MMI coupler designs with shorter lengths and higher normalized access waveguides offer better manufacturing tolerances and optical bandwidths. Novel bar butterfly MMI couplers are more compact than conventional designs and offer a better imbalance response in a larger wavelength range, although slightly higher excess losses are expected. Footprints from  $1.8 \times 11.5 \mu\text{m}^2$  to  $7.2 \times 29.6 \mu\text{m}^2$  are obtained. MMI couplers are

manufactured using state-of-the-art CMOS manufacturing processes with sub-nanometer lithographic precision. It has been shown that CMOS layer thicknesses tolerances of 5% can induce additional excess loss of around 0.5dB. Due to the high contrast ratio of these waveguides 3D-FDTD simulations are performed to get accurate designs.

## 5. ACKNOWLEDGEMENT

This work has been sponsored by the Spanish institutions Ministerio de Economía y Competitividad under project TEC2012-37983-C03-02, and grant EEBB-1-13-07511, Ministerio de Educación under grant PRX12/00007 and Fundación Caja Madrid.

## REFERENCES

- [1] Orcutt, J.S, Anatol Khilo, A., Holzwarth, C. W., et al. J. R. Ram, "Nanophotonic integration in state-of-the-art CMOS foundries," *Optics Express*, 19, 2335 (2011)
- [2] Meade, Roy; Tehar-Zahav, Ofer; Sternberg, Zvi; Megged, Efraim; Sandhu, Gurtej; Orcutt, Jason S.; Ram, Rajeev; Stojanovic, Vladimir; Michael, R.; Timurdogan, Erman; Shainline, Jeffrey; Popovic, Milos, "Integration of silicon photonics in a bulk CMOS memory flow," *Optical Interconnects Conference, 2013 IEEE* , 114 (2013)
- [3] P. A. Besse, M. Bachmann, H. Melchior, L. B. Soldano, and M. K. Smit, "Optical Bandwidth and Fabrication Tolerances of Multimode Interference Couplers," *IEEE Journal of Light Technology*, 12 (6), 1004 (1994)
- [4] P. Dong, C. Xie, L. Chen, N. K. Fontaine, and Y. Chen, "Experimental demonstration of microring quadrature phase-shift keying modulators," *Optics Letters*, 37 (7), 1178 (2012)
- [5] D. Xu, A. Densmore, P. Waldron, J. Lapointe, E. Post, A. Delâge, S. Janz, P. Cheben, J. H. Schmid and B. Lamontagne, "High bandwidth SOI photonic wire ring resonators using MMI couplers," *Optics Express*, 15 (6), 3149 (2007)
- [6] Leuthold et al, "Multimode Interference Couplers with Tunable Power Splitting Ratios," *Journal of Lightwave Technology*, 19 (5), 700 (2001)
- [7] F. Wang, J. Yang, L. Chen, X. Jiang, and M. Wang, "Optical Switch Based on Multimode Interference Coupler," *Photonics Technology Letters*, 18 (2), 421 (2006).
- [8] C. Vázquez, F. J. Mustieles, y J. F. Hernández Gil, "Three-Dimensional Method for Simulation of Multimode Interference Couplers," *Journal of Lightwave Technology*, 13, 2296 (1995)
- [9] Bachmann et al, "Overlapping-image multimode interference couplers with a reduced number of self-images for uniform and nonuniform power splitting," *Applied Optics*, 34 (30), 6898 (1995)
- [10] Soldano et al, "Planar Monomode Optical Couplers Based on Multimode Interference Effects Planar Monomode Optical Couplers Based on Multimode Interference Effects," *Journal of Lightwave Technology*, 10 (12), 1843 (1992).
- [11] Martin T. Hill, X. J. M. Leijtens, G. D. Khoe, and M. K. Smit "Optimizing imbalance and loss in 2x2 3dB multimode interference couplers via access waveguide width," *Journal of Lightwave Technology*, 21 (10), 2305 (2003)
- [12] Besse et al, "New 2x2 and 1x3 Multimode Interference Couplers with Free Selection of Power Splitting Ratios," *Journal of Lightwave Technology*, 14 (10), 2286 (1996).
- [13] L. B. Soldano and Erik C. M. Pennings, "Optical Multi-Mode Interference Devices Based on Self-Imaging : Principles and Applications," *Journal of Lightwave Technology*, 13 (10), 615 (1995).
- [14] M. T. Hill, X. J. M. Leijtens, G. D. Khoe, and M. K. Smit, "Optimizing Imbalance and Loss in 2x2 3-dB Multimode Interference Couplers via Access Waveguide Width," *Journal of Light Technology*, 21 (10), 2305 (2003).
- [15] Z. Sheng, Z. Wang, C. Qiu, L. Li, A. Pang, A. Wu, X. Wang, S. Zou, F. Gan, "A Compact and Low-Loss MMI Coupler Fabricated With CMOS Technology," *IEEE Photonics Journal*, 4 (6), (2012).
- [16] C. M. Weinert and N. Agrawal, "Three-Dimensional Finite Difference Simulation of Coupling Behavior and Loss in Multimode Interference Devices," *IEEE Photonics Technology Lett*, 1 (5), (1995).